

REPORTS

12. T. I. Gerasimova, D. A. Gdula, D. V. Gerasimov, O. Simonova, V. G. Corces, *Cell* **82**, 587 (1995).
13. T. I. Gerasimova, V. G. Corces, *Cell* **92**, 511 (1998).
14. J. Mihaly *et al.*, *Cell. Mol. Life Sci.* **54**, 60 (1998).
15. K. Hagstrom, M. Müller, P. Schedl, *Genes Dev.* **10**, 3202 (1996).
16. J. Zhou, S. Barolo, P. Szymanski, M. Levine, *Genes Dev.* **10**, 3195 (1996).
17. J. Zhou, M. Levine, *Cell* **99**, 567 (1999).
18. S. Qian, B. Varjavand, V. Pirrotta, *Genetics* **131**, 79 (1992).
19. P. Georgiev, M. Kozycina, *Genetics* **142**, 425 (1996).
20. The transposon constructs were based on the CaSpeR series and derivatives. The entire yellow gene was con-

tained in an 8-kb fragment with the partially overlapping body and wing enhancers located, respectively, at positions -1266 to -1963 and -1808 to -2873 from the transcription start site. The white Eye enhancer fragment contained eye and testis enhancers (18). The Su(Hw) insulator was a 430-bp fragment containing 12 Su(Hw) binding sites, amplified by polymerase chain reaction from the gypsy retrotransposon. Details of the constructions are available upon request. The constructs were injected in γ -ac-w¹¹¹⁸ embryos, and the transgenic flies were identified by their eye color. The transformed lines were tested by Southern blot hybridization for transposon integrity, copy number, and presence of the enhancers and Su(Hw) insulators. Only lines with single-copy

- inserts were used. Lines in a *su(Hw)*⁻ mutant background were obtained by consecutively crossing transgenic males with *C(1)RM,yf; D1 T(2;3)Xa*, *C(1)RM,yf; su(Hw)/T(2;3)Xa*, *C(1)RM,yf; su(Hw)²sbdl/T(2;3)Xa* females as described (19).
21. Supported by grants from the Human Frontiers Science Program and from INTAS to P.G. and V.P. P.G. was an International Research Scholar of the Howard Hughes Medical Institute and received an award from the Volkswagen Stiftung Foundation, and A.G. was supported by a stipend from the Center for Medical Studies, University of Oslo.

4 October 2000; accepted 19 December 2000

Crystal Structure of an Initiation Factor Bound to the 30S Ribosomal Subunit

Andrew P. Carter,¹ William M. Clemons Jr.,¹
Ditlev E. Brodersen,¹ Robert J. Morgan-Warren,¹
Thomas Hartsch,² Brian T. Wimberly,¹ V. Ramakrishnan^{1*}

Initiation of translation at the correct position on messenger RNA is essential for accurate protein synthesis. In prokaryotes, this process requires three initiation factors: IF1, IF2, and IF3. Here we report the crystal structure of a complex of IF1 and the 30S ribosomal subunit. Binding of IF1 occludes the ribosomal A site and flips out the functionally important bases A1492 and A1493 from helix 44 of 16S RNA, burying them in pockets in IF1. The binding of IF1 causes long-range changes in the conformation of H44 and leads to movement of the domains of 30S with respect to each other. The structure explains how localized changes at the ribosomal A site lead to global alterations in the conformation of the 30S subunit.

The synthesis of functional polypeptides requires initiation of translation to occur at the correct mRNA codon. In prokaryotes, selection of the start codon involves formation of a 30S initiation complex containing the small (30S) ribosomal subunit, three protein initiation factors (IF1, IF2, and IF3), and initiator tRNA (formyl-methionine-tRNA^{Met}) base-paired to the mRNA start codon in the ribosomal P site (1–3). IF3 acts to ensure that the 30S subunit dissociates from the large (50S) ribosomal subunit (4). It also cooperates with IF2 to prevent incorrect P-site interactions by ensuring that only initiator tRNA is present in the P site (5–7) and that it interacts only with the start codon (8). The 50S subunit binds the 30S initiation complex after IF3 has been displaced, triggering hydrolysis of the guanosine 5'-triphosphate (GTP) bound to IF2. Subsequently, IF2 is released, allowing initiator tRNA to form the first peptide bond with the first elongator aminoacyl tRNA (aa-tRNA), which is deliv-

ered to the A site in complex with the elongation factor EF-Tu.

The role of IF1 is the least well defined of the three initiation factors (2). It has been implicated in subunit dissociation preceding initiation (4, 9), stimulating 30S complex formation (10, 11), release of IF2 from the 70S (12, 13), and blocking of the A site to tRNA binding (3, 14). The gene encoding IF1 is essential in *Escherichia coli* (15), suggesting that one or more of its functions are crucial in vivo. Here we present a 3.2 Å resolution crystal structure of the complex of IF1 with the 30S ribosomal subunit from *Thermus thermophilus*. The structure allows us to discuss the functions of IF1 at a molecular level and also provides an atomic resolution view of factor-induced conformational changes occurring within the small ribosomal subunit.

The large solvent channels found in the 30S subunit crystal form made it possible to soak IF1 directly into crystals prepared as described previously (16, 17). Diffraction data extending to 3.2 Å were collected from these crystals (Table 1), and a single round of refinement against the native 30S coordinates resulted in a model with R/R_{free} of (0.239/0.278). The electron density for IF1 was visible in σ_A -weighted $2mF_o - DF_c$ maps (Fig. 1A). The nuclear magnetic resonance (NMR)

structure of *E. coli* IF1 (18) was unambiguously placed in the density and rebuilt with the sequence of the *T. thermophilus* protein (Fig. 1). The C α root-mean-square deviation between our final refined structure and the NMR structure is 1.41 Å. The major changes in the 30S structure occurred in helix 44 (H44), although small shifts in the relative positions of the RNA domains were also observed. The statistics of a final round of refinement including IF1 are shown in Table 1.

IF1 is a member of the S1 family of OB fold proteins (19, 20), consisting of a barrel of five β strands with the loop between strands 3 and 4 capping one end of the barrel (18). It binds to the 30S subunit in a cleft formed between H44, the 530 loop, and protein S12 (Fig. 2, A and B). The face of IF1 that interacts with the ribosome is rich in basic residues, whereas most of the acidic residues are on the solvent-exposed surface. This highly asymmetric charge distribution is probably important in stabilizing binding to the 30S subunit. Conserved residues in IF1 make tight electrostatic and hydrogen bonding interactions with the phosphate backbone of the 530 loop. A loop from IF1 inserts into the minor groove of H44, forms contacts with the backbone of several nucleotides, and flips out bases A1492 and A1493 (Fig. 2A). A1493 is buried in a pocket on the surface of IF1, whereas A1492 sits in a cavity formed at the interface between IF1 and S12 (Fig. 2D). In both cases conserved arginine residues (Arg⁴⁶ and Arg⁴¹, respectively) are in a position to stack against the bases and stabilize the interaction. In contrast to the antibiotic paromomycin, which flips out A1492 and A1493 so that they are stacked together (21), IF1 causes them to be splayed apart.

The structure agrees well with most biochemical and mutagenesis data. The sequestering of bases A1492 and A1493 into protein pockets explains why IF1 completely protects them from chemical modification (14). The abolition of IF1 binding in A1492G or A1493G mutants is consistent with the bulkier guanine base being unable to fit in either binding pocket (22). The increase in reactivity of A1408 (14) is explained by the disruption of the base pair it makes with A1493 in the native structure (16, 23). Finally, muta-

¹Medical Research Council Laboratory of Molecular Biology, Hills Road, Cambridge CB2 2QH, UK. ²Göttingen Genomics Laboratory, Institut für Mikrobiologie und Genetik, Georg-August-Universität Göttingen, Grisebachstr. 8, D-37077 Göttingen, Germany.

*To whom correspondence should be addressed. E-mail: ramak@mrc-lmb.cam.ac.uk

REPORTS

tion of His³⁵ to Asp in *E. coli* IF1 abolishes 30S binding (24), which is consistent with the observation that the equivalent residue in *Thermus* (Tyr³⁵) makes hydrogen bonding interactions with the phosphate backbone of C519. Further details of the IF1-30S interactions are described in the supplementary material (25).

The locations of the A, P, and E sites on the 30S subunit (Fig. 2C) have been inferred from a superposition (21) based on the 7.8 Å crystal structure of the whole 70S ribosome in complex with mRNA and tRNAs (26). The positions of the tRNAs suggest that IF1 would sterically block tRNA binding to the A site (Fig. 2, B and C). This agrees with a previous proposal based on the observation that IF1 protects the same bases as A-site tRNA (14). IF1 covers, but does not block, a channel at the base of the A site through which mRNA could pass (27). The surface charge distribution on IF1 and the manner in which A1492 and A1493 interact with it suggest that it does not directly mimic the A-site tRNA.

The significance of A-site occlusion by IF1 is not yet understood. It has been proposed to be important in ensuring that free aa-tRNA does not bind in the A site during initiation (14). In the absence of the 50S, the EF-Tu-coupled proofreading activity would not function, so that tRNA binding in the A site could result in a higher level of miscoding. It is also possible that in the presence of IF2, the higher affinity of tRNA for the P site over the A site is not sufficient to direct initiator tRNA solely into the P site unless the A site is blocked by IF1(3).

However, the location of IF1 on the ribosome may also relate to its interaction with IF2. The interaction of IF1 and IF2 is supported by biochemical data (3, 28, 29), and although the full significance of the contacts is not clear, two explanations can be proposed. First, in the absence of IF1, the domains of IF2 may not be in the correct conformation to correctly position initiator tRNA in the P site. This could explain the stimulatory effect of IF1 on 30S initiation complex formation (10, 11). Second, the interaction may be important for the role of IF1 in aiding release of IF2 from the 70S subunit (12, 13). A full understanding of the interaction between IF1 and IF2 will require a structure of both factors in complex with the ribosome.

In addition to the localized changes around A1492 and A1493, IF1 binding to the 30S subunit also causes conformational changes in H44 over a distance of about 70 Å (Fig. 3A) and moreover leads to small but significant shifts in the relative positions of the domains of the subunit. In H44, nucleotides C1411 and C1412 (strand A, Fig. 3A) move laterally by 5 Å, in order to make electrostatic interactions with Arg⁶⁴ from IF1

and Arg⁴¹ from S12 (Fig. 3, B and C). This movement causes a concerted displacement in the position of backbone phosphates of

A1413-C1420 with respect to the axis of H44 (Fig. 3A). Nucleotides on the complementary strand (strand B, Fig. 3A) do not move much

Table 1. Summary of crystallographic data.

Data collection:

| Beam-line | Resolution limit (Å) | No. of observations | No. of unique reflections | Completeness (%) | | $\langle I \rangle / \langle \sigma \rangle$ | | R_{sym} (%) | |
|---|----------------------|---------------------|---------------------------|------------------|-------------|--|-------------|----------------------|-------------|
| | | | | Overall | Outer shell | Overall | Outer shell | Overall | Outer shell |
| ID14-4 | 3.2 | 854,384 | 227,537 | 96.2 | 92.2 | 5.1 | 1.9 | 14.0 | 49.9 |
| Refinement: | | | | | | | | | |
| Resolution range | | | | 99.0–3.2 Å | | | | | |
| Reflections excluded for cross-validation | | | | 5% | | | | | |
| Number of nonhydrogen atoms | | | | | | | | | |
| Proteins | | | | 19,896 | | | | | |
| RNA | | | | 32,283 | | | | | |
| Metals | | | | 67 | | | | | |
| R factor (conventional) | | | | 0.218 | | | | | |
| R factor (free) | | | | 0.261 | | | | | |
| Cross-validated σ_A coordinate error | | | | 0.56 Å | | | | | |
| Deviations from ideality | | | | | | | | | |
| rms deviations in bond lengths | | | | 0.007 Å | | | | | |
| rms deviations in bond angles | | | | 1.25° | | | | | |

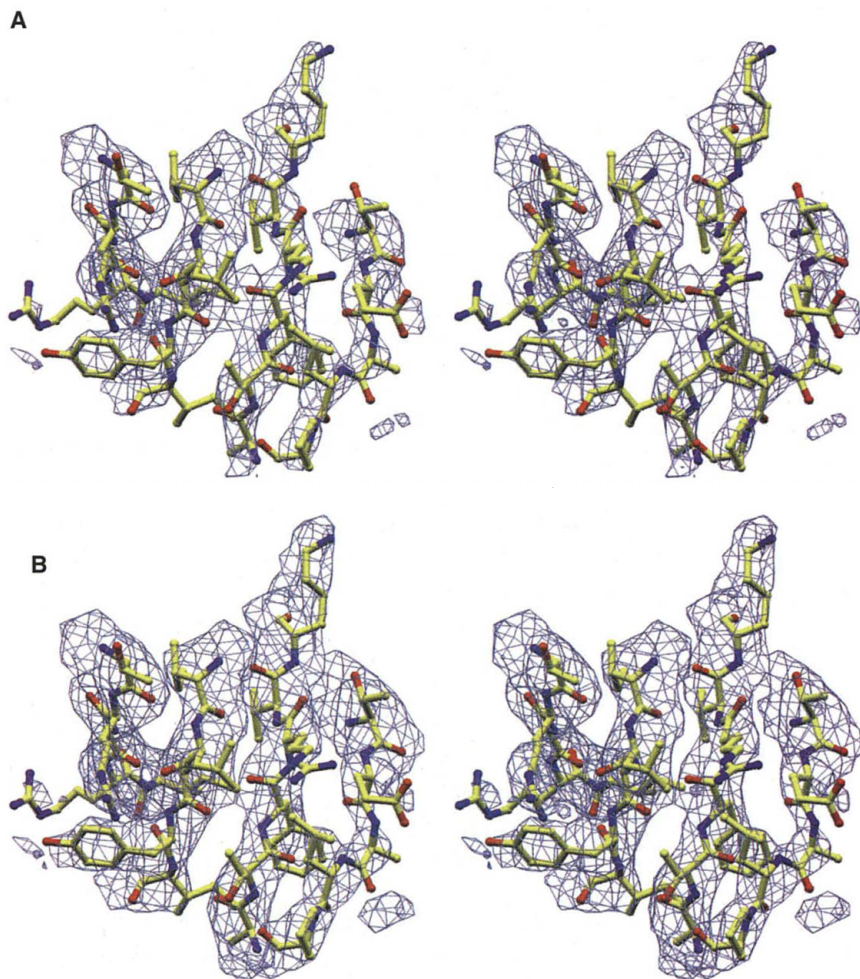


Fig. 1. Stereo views of electron density maps of the 30S-IF1 complex, showing a β sheet in IF1. (A) σ_A -weighted $2mF_o - DF_c$ maps from an initial refinement in which no model for IF1 was included. (B) The corresponding maps after refinement with IF1.

REPORTS

with respect to the helical axis, which results in disruption of base pairing. In particular, the noncanonical A1413-G1487 base pair is broken on IF1 binding (Fig. 3, B and C), which accounts for the increased reactivity of both bases to chemical modification in the presence of IF1 (22). These bases belong to the "class III" sites which are known to be protected by tRNA and some antibiotics (30). Further down H44 (asterisk in Fig. 3A), nu-

cleotides in strand B move with respect to the helical axis, whereas the positions of those in strand A remain relatively unchanged.

In addition to the changes in H44, IF1 causes a movement of the domains of the 30S with respect to each other. The head, platform, and shoulder all rotate toward the A site. In contrast, the presence of three antibiotics (streptomycin, paromomycin, and spectinomycin) (21) causes the platform and

shoulder to tilt toward the A site, but the head to tilt back, away from it. Two animations showing these changes are available in the supplementary material (25). Although small (changes of up to 1.2 Å in a model with a σ_A -weighted coordinate error of 0.54 Å), the concerted nature of the changes suggests they are significant. It is possible that in the absence of crystal lattice constraints a similar but more extensive movement of the domains

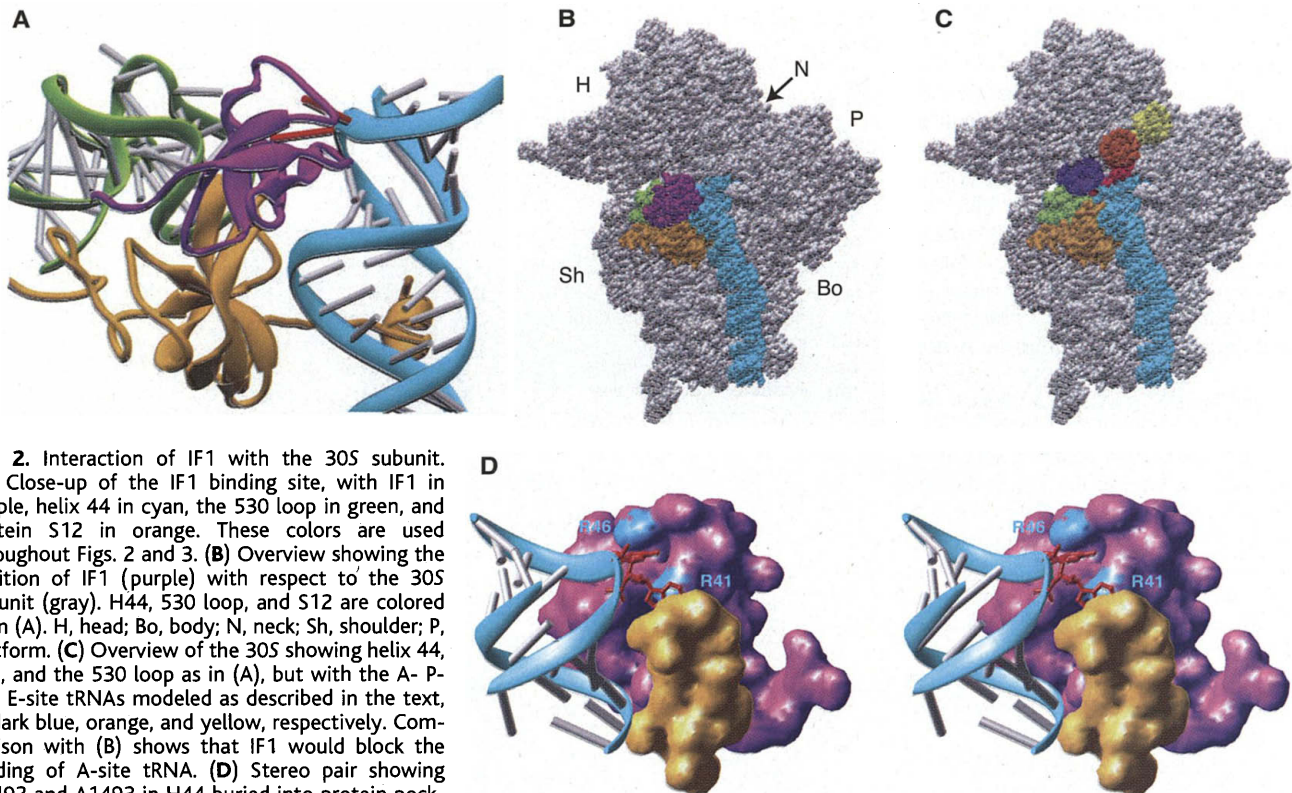


Fig. 2. Interaction of IF1 with the 30S subunit. (A) Close-up of the IF1 binding site, with IF1 in purple, helix 44 in cyan, the 530 loop in green, and protein S12 in orange. These colors are used throughout Figs. 2 and 3. (B) Overview showing the position of IF1 (purple) with respect to the 30S subunit (gray). H44, 530 loop, and S12 are colored as in (A). H, head; Bo, body; N, neck; Sh, shoulder; P, platform. (C) Overview of the 30S showing helix 44, S12, and the 530 loop as in (A), but with the A-, P- and E-site tRNAs modeled as described in the text, in dark blue, orange, and yellow, respectively. Comparison with (B) shows that IF1 would block the binding of A-site tRNA. (D) Stereo pair showing A1492 and A1493 in H44 buried into protein pockets formed by IF1 and a combination of IF1 and S12.

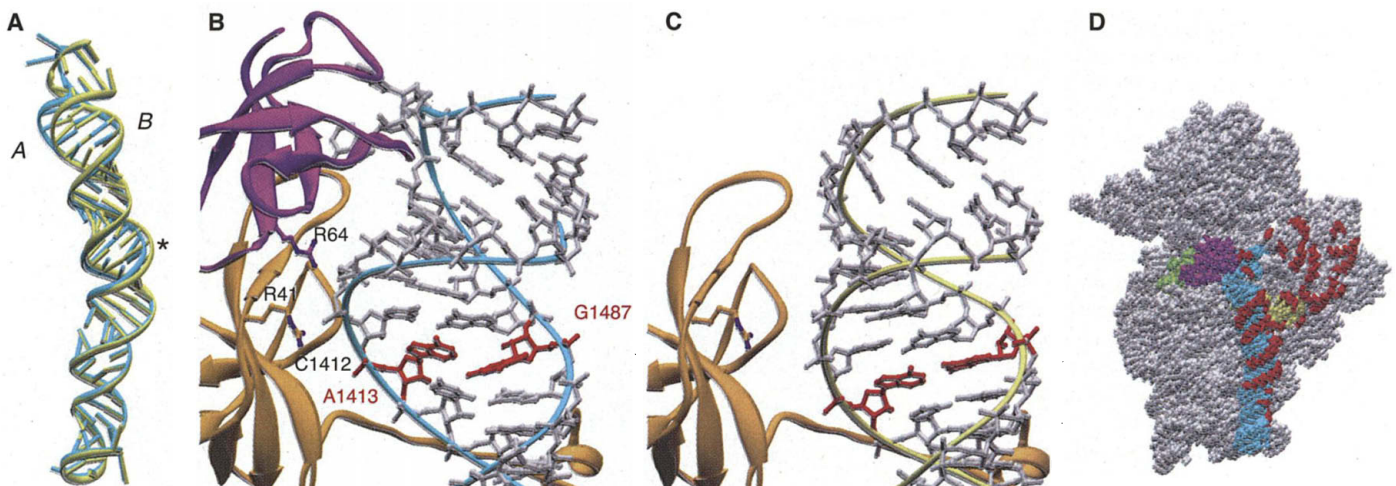


Fig. 3. Conformational changes in the 30S on IF1 binding. (A) Helix 44 in the presence (cyan) and absence (yellow) of IF1, showing significant distortions of the helix. (B) Close-up showing how IF1 and S12 together can distort helix 44. The backbone moves so much that the noncanonical base pair between A1413 and G1487 is broken. (C) The

same region in the absence of IF1, showing a more regular helix and the intact base pair between A1413 and G1487. (D) Surface of the 30S subunit with IF1 bound, showing regions that are protected by association with the 50S subunit in red (see text). Helix 44 and the 530 loop are also shown.

REPORTS

would be observed, as was suggested for bacteriorhodopsin (31). A larger movement of the head could explain how the base G530, which remains exposed in the structure, is protected from chemical modification by IF1 (14).

IF1 increases the rate at which 30S subunits associate and dissociate with 50S, but does not shift the equilibrium between 70S ribosomes and free subunits (4). This effect was demonstrated by showing that IF1 increases the rate of incorporation of radiolabeled 50S subunits into unlabeled 70S ribosomes (32). In the presence of IF3, which blocks subunit association (4), the effect of IF1 is to increase the degree of subunit dissociation beyond that observed for IF3 alone. This role of IF1 is likely to be significant in vivo because the concentration of IF3 is some 100-fold less (2) than that required to dissociate ribosomes fully in vitro (33).

H44 makes extensive contacts with the 50S subunit (26, 34) (Fig. 3D). It is possible that the conformation of H44 in the presence of IF1 resembles its conformation during the transition state of subunit interaction. Stabilization of this transition state would cause an increase in the rate of both subunit dissociation and association. However, the effect of IF1 on dissociation could also be the result of other structural changes in regions of the 30S subunit that contact the 50S subunit, such as the head domain.

Insertion of the loop of IF1 into H44 and flipping out the bases A1492 and A1493 destabilize the top of the helix, which allows nucleotides C1411 and C1412 to move to interact with a binding site formed by proteins IF1 and S12. The movement of C1411 and C1412 shifts one strand of the helix with respect to the other, and this in turn propagates changes in conformation over a long distance. In addition, H44 is connected directly to the head of the 30S subunit, and changes in its conformation appear to be directly related to movement of this domain. Changes in H44 coupled with the movement

of domains have also been observed by cryo-electron microscopy of various functional states of the ribosome (35–37). It will be interesting to see whether these other changes in the 30S subunit resemble those seen here in the presence of IF1.

References and Notes

1. C. B. Gualerzi et al., in *The Ribosome, Function, Antibiotics, and Cellular Interactions*, R. A. Garrett, S. R. Douthwaite, A. Liljas, A. T. Matheson, P. B. Moore, H. F. Noller, Eds. (American Society for Microbiology, Washington, DC, 2000), pp. 477–494.
2. C. O. Gualerzi, C. L. Pon, *Biochemistry* **29**, 5881 (1990).
3. S. Brock, K. Szkaradkiewicz, M. Sprinzl, *Mol. Microbiol.* **29**, 409 (1998).
4. T. Godfrey-Colburn et al., *J. Mol. Biol.* **94**, 461 (1975).
5. D. Hartz, J. Binkley, T. Hollingsworth, L. Gold, *Genes Dev.* **4**, 1790 (1990).
6. M. A. Canonaco, R. A. Calogero, C. O. Gualerzi, *FEBS Lett.* **207**, 198 (1986).
7. X. Q. Wu, U. L. RajBhandary, *J. Biol. Chem.* **272**, 1891 (1997).
8. T. Meinel, C. Sacerdot, M. Graffe, S. Blanquet, M. Springer, *J. Mol. Biol.* **290**, 825 (1999).
9. D. Dottavio-Martin, D. P. Suttle, J. M. Ravel, *FEBS Lett.* **97**, 105 (1979).
10. C. L. Pon, C. O. Gualerzi, *FEBS Lett.* **175**, 203 (1984).
11. W. Wintermeyer, C. Gualerzi, *Biochemistry* **22**, 690 (1983).
12. R. Benne, N. Naaktgeboren, J. Gubbens, H. O. Voorma, *Eur. J. Biochem.* **32**, 372 (1973).
13. E. A. Stringer, P. Sarkar, U. Maitra, *J. Biol. Chem.* **252**, 1739 (1977).
14. D. Moazed, R. R. Samaha, C. Gualerzi, H. F. Noller, *J. Mol. Biol.* **248**, 207 (1995).
15. H. S. Cummings, J. W. Hershey, *J. Bacteriol.* **176**, 198 (1994).
16. B. T. Wimberly et al., *Nature* **407**, 327 (2000).
17. The gene for IF1 from *T. thermophilus* was introduced into the vector pET13a (38) and expressed in B834 (DE3) cells. *Escherichia coli* proteins were precipitated from induced cell lysates (39) by addition of a volume of boiling lysis buffer to bring the final temperature up to ~70°C. IF1 was further purified by ion-exchange and hydroxylapatite chromatography as described (40), except that buffers for the two steps were at pH 6.8 and 6.5, respectively. Buffer exchange and protein concentration were carried out in Ultra-free filters; 30S crystals were prepared as described (16). After equilibration in 26% 2-methyl-2,4-pentanediol (MPD), crystals were transferred into 26% MPD containing 80 μM IF1 for 24 hours before flash-cooling in liquid nitrogen. Data were collected on beamline ID14-4 at the European Synchrotron Radiation Facility (ESRF) in Grenoble, France, and integrated and scaled with HKL-2000 (41). The re-

finer 3 Å structure of the 30S subunit (16) with the cobalt ions removed was used as a starting model for refinement with CNS (42) as described (21). Detailed methods are given in the supplementary material (25).

18. M. Sette et al., *EMBO J.* **16**, 1436 (1997).
19. M. Bycroft, T. J. Hubbard, M. Proctor, S. M. Freund, A. G. Murzin, *Cell* **88**, 235 (1997).
20. M. Gribnikov, *Gene* **119**, 107 (1992).
21. A. P. Carter et al., *Nature* **407**, 340 (2000).
22. K. D. Dahlquist, J. D. Puglisi, *J. Mol. Biol.* **299**, 1 (2000).
23. D. Fourmy, S. Yoshizawa, J. D. Puglisi, *J. Mol. Biol.* **277**, 333 (1998).
24. C. O. Gualerzi et al., *Protein Eng.* **3**, 133 (1989).
25. Supplementary data are available at Science Online at www.sciencemag.org/cgi/content/full/291/5503/498/DC1.
26. J. H. Cate, M. M. Yusupov, G. Z. Yusupova, T. N. Earnest, H. F. Noller, *Science* **285**, 2095 (1999).
27. K. R. Lata et al., *J. Mol. Biol.* **262**, 43 (1996).
28. J. M. Moreno, L. Drskjotersen, J. E. Kristensen, K. K. Mortensen, H. U. Sperling-Petersen, *FEBS Lett.* **455**, 130 (1999).
29. G. Boileau, P. Butler, J. W. Hershey, R. R. Traut, *Biochemistry* **22**, 3162 (1983).
30. D. Moazed, H. F. Noller, *Nature* **327**, 389 (1987).
31. S. Subramaniam, R. Henderson, *Nature* **406**, 653 (2000).
32. M. Noll, H. Noll, *Nature New Biol.* **238**, 225 (1972).
33. J. P. McCutcheon et al., *Proc. Natl. Acad. Sci. U.S.A.* **96**, 4301 (1999).
34. C. Merryman, D. Moazed, J. McWhirter, H. F. Noller, *J. Mol. Biol.* **285**, 97 (1999).
35. I. S. Gabashvili et al., *EMBO J.* **18**, 6501 (1999).
36. J. Frank, R. K. Agrawal, *Nature* **406**, 319 (2000).
37. M. S. VanLoock et al., *J. Mol. Biol.* **304**, 507 (2000).
38. S. E. Gerchman, V. Graziano, V. Ramakrishnan, *Protein Expr. Purif.* **5**, 242 (1994).
39. J. H. Kycia et al., *Biochemistry* **34**, 6183 (1995).
40. B. T. Wimberly, S. W. White, V. Ramakrishnan, *Structure* **5**, 1187 (1997).
41. Z. Otwinowski, W. Minor, in *Methods in Enzymology*, C. W. J. Carter, R. M. Sweet, Eds. (Academic Press, New York, 1997), vol. 276, pp. 307–325.
42. A. T. Brünger et al., *Acta Crystallogr. D Biol. Crystallogr.* **54**, 905 (1998).
43. We thank M. Pacold and J. Ogle for critical comments on the manuscript and R. Ravelli, S. McSweeney, and G. Leonard for help and advice during synchrotron data collection at ESRF, Grenoble, France. Supported by the Medical Research Council (U.K.) and grant GM 44973 from the NIH (S. W. White and V.R.) and by a Human Frontier Science Program long-term postdoctoral fellowship (D.E.B.) and an NIH predoctoral fellowship (W.M.C.). Coordinates have been deposited in the Protein Data Bank with the accession number 1HR0.

27 November 2000; accepted 20 December 2000
Published online 4 January 2001; 10.1126/science.1057766
Include this information when citing this paper.

Enhance your AAAS membership with the Science Online advantage.

- **Full text Science**—research papers and news articles with hyperlinks from citations to related abstracts in other journals before you receive *Science* in the mail.
- **ScienceNOW**—succinct, daily briefings, of the hottest scientific, medical, and technological news.
- **Science's Next Wave**—career advice, topical forums, discussion groups, and expanded news written by today's brightest young scientists across the world.

Science ONLINE

- **Research Alerts**—sends you an e-mail alert every time a *Science* research report comes out in the discipline, or by a specific author, citation, or keyword of your choice.
- **Science's Professional Network**—lists hundreds of job openings and funding sources worldwide that are quickly and easily searchable by discipline, position, organization, and region.
- **Electronic Marketplace**—provides new product information from the world's leading science manufacturers and suppliers, all at a click of your mouse.

All the information you need....in one convenient location.

Visit Science Online at <http://www.sciencemag.org>, call 202-326-6417, or e-mail membership2@aaas.org for more information.

AAAS is also proud to announce site-wide institutional subscriptions to Science Online. Contact your subscription agent or AAAS for details.

 AMERICAN ASSOCIATION FOR THE ADVANCEMENT OF SCIENCE